6. Atmospheric Mixing

Previous chapters have dealt solely with transport in various water bodies and have presented examples of one-dimensional solutions to the transport equations. We now turn our attention to transport and mixing in the atmosphere, and by necessity, we will have to give more attention to three-dimensional solutions. Because of the atmosphere's unique composition and boundary and forcing conditions, atmospheric turbulence is more complicated than the idealized homogeneous, stationary, isotropic case. Moreover, these complications impact transport and mixing because they determine the values of the turbulent diffusion and dispersion coefficients. Hence, a concise discussion of atmospheric mixing requires also studying atmospheric turbulence and the resulting modifications in the behaviour of mixing coefficients from the idealized case.

This chapter begins with an introduction to atmospheric turbulence and a review of turbulent boundary layer structure. The log-velocity profile for a turbulent shear flow is introduced, and the behaviour of turbulence throughout a neutrally stable atmospheric boundary layer is described. Because of their importance to turbulence characteristics, the buoyancy effects of heating and cooling within the boundary layer are discussed qualitatively. The discussion on mixing begins with a review of turbulent mixing in three-dimensional, homogeneous, stationary turbulence. The solution for a continuous point source is derived and used to illustrate mixing in the remaining section. The chapter closes by adapting the idealized solution in homogeneous, stationary turbulence to the turbulence present in the atmosphere.

Much of the material in this chapter was taken from Csanady (1973) and from Fedorovich (1999). For further reading, those two sources are highly recommended, along with the classic books by Lumley & Panofsky (1964) and Pasquill (1962) and more recent contributions by Garratt (1992) and Kaimal & Finnigan (1994).

6.1 Atmospheric turbulence

In Environmental Fluid Mechanics, we are concerned with local mixing processes in fluids that interact with living organisms. For the atmosphere, this means that we are interested in mixing processes near the earth's surface. Because of the no-slip boundary condition at the surface, wind in the upper atmosphere generates a near-surface boundary layer, defined by variations in velocity and often accompanied by variations in temperature (and density). Figure 6.1 shows this situation schematically. Because of its dominant role in

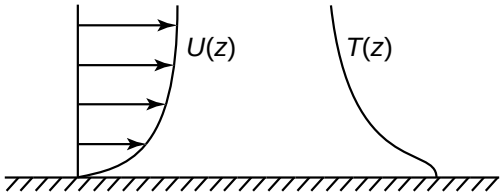

Fig. 6.1. Schematic of the velocity and temperature variation within the atmosphere near the earth's surface. The region of high velocity shear is called a boundary layer.

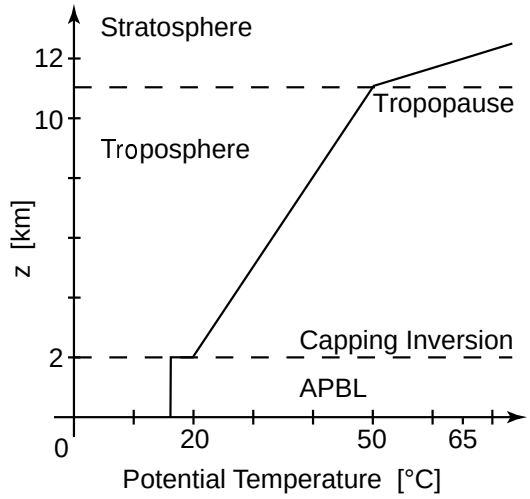

Fig. 6.2. Schematic of the potential temperature profile in the earth's troposphere and lower stratosphere showing the atmospheric planetary boundary layer (APBL).

mixing near the earth's surface, we present here a short introduction to turbulence in the atmospheric boundary layer.

6.1.1 Atmospheric planetary boundary layer (APBL)

Fedorovich (1999) defines the atmospheric planetary boundary layer (APBL) as the subdomain of the lower portion of the earth's planetary atmosphere (troposphere) which is in contact with the bottom boundary (earth's surface) and which varies in depth from several meters to a few kilometers. Figure 6.2 provides a schematic of this definition. The figure depicts the APBL as the lower part of the troposphere and shows that it is separated from the linearly stratified region of the troposphere by a strong density gradient, called the capping inversion. The capping inversion arises due to strong mixing that occurs at the earth's surface which results in a weaker density gradient within the APBL than in the upper troposphere. Although the density gradient shown in the figure is for a neutral APBL (no density gradient), heating and cooling processes within the APBL can lead to both unstable and stable conditions, discussed below under buoyancy effects. Above the APBL, the wind has an approximately constant velocity; hence, the APBL encompasses the full near-surface boundary layer.

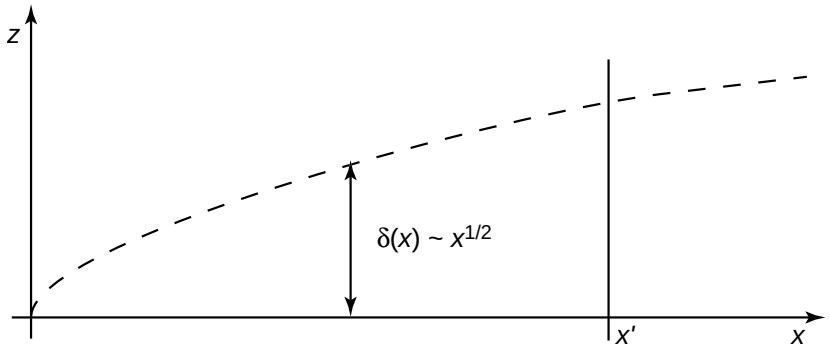

(a.) Growth of a boundary layer with increasing fetch.

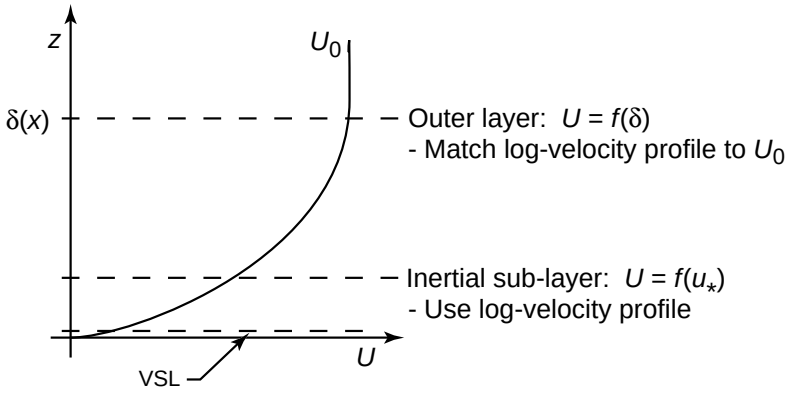

(b.) Boundary layer structure at the section x'.

Fig. 6.3. Schematic of the development of a turbulent boundary layer over a flat surface.

6.1.2 Turbulent properties of a neutral APBL

Figure 6.3 shows the development of a general turbulent boundary layer over a flat surface. In the upper figure, the boundary layer is tripped at $x = 0$ and begins to grow in height downstream as an increasing function of $x^{1/2}$. In the idealized case, the boundary layer is tripped by the edge of a flat plate extending into a free turbulent flow. In nature, boundary layers start in response to changes in friction (roughness), as when the wind blows over a long, smooth lake and suddenly encounters a forest on the other side. The distance the wind has blown downstream of a major change in surface properties is called the fetch.

A turbulent boundary layer at any point x contains three major zones that differ in their turbulence characteristics (refer to Figure 6.3(b.)). The lowest layer, directly in contact with the surface, is the viscous sub-layer (VSL). It has a depth of about $5\nu/u_*$ (of order millimeter in the atmosphere). The VSL thickness is independent of the total boundary layer depth $\delta(x)$, and velocities in the VSL are low so that the flow is laminar. A transition to turbulence occurs between $5\nu/u_*$ and $50\nu/u_*$. Above this transition zone, and to a height of about 10-20% of the total boundary layer depth (of order 100 m in the atmosphere), lies the inertial sub-layer (ISL), also called the Prandtl layer in the atmosphere. The inertial sub-layer is fully turbulent, and turbulent properties

are functions of the friction velocity only (i.e. they are independent of the total boundary layer depth). The mean longitudinal velocity profile in the ISL is given by the well-known log-velocity profile

$$\frac{U(z)}{u_*} = \frac{1}{\kappa} \ln\left(\frac{u_* z}{\nu}\right) + C \tag{6.1}$$

where $\kappa \approx 0.4$ is the von Karman constant and C is an integration constant about equal to five. It is important to note that within this layer $U(z)$ is independent of $\delta(x)$. The remaining region of the boundary layer is called the outer layer, or Ekman layer in the atmosphere, and extends up to where the velocity becomes U_0. Within the atmosphere, the Ekman layer is deep enough that it experiences Coriolis effects due to the earth's rotation. In the outer layer, turbulence properties and the velocity profile are dependent on the total layer depth, and we use a technique called matching to adjust the log-velocity profile in this layer so that it reaches U_0 at $z = \delta(x)$.

In general, turbulence measurements in the APBL depend on the height of the measurement, the roughness of the ground, and the stability (Csanady 1973). Measurements near the surface (within the ISL) demonstrate that

$$u_{rms} \propto u_* \tag{6.2}$$

where $u_{rms} = (\overline{u'^2})^{1/2}$. Above this surface layer, u_{rms} tends to decay with height. Because the land surface is quite rough in comparison to an idealized flat plate, the log-velocity profile cited above is adjusted in the ISL to give

$$U(z) = \frac{u_*}{\kappa} \ln\left(\frac{z}{z_0}\right) \tag{6.3}$$

where z_0 is the roughness height (valid for $z \gg z_0$).

Because the mean wind-speed increases with height and the turbulent fluctuation velocities are constant with height within the neutral APBL, turbulence intensity decreases with height. Turbulence intensity is defined as

$$i_x = \frac{(\overline{u'^2})^{1/2}}{U(z)} \tag{6.4}$$

$$i_y = \frac{(\overline{v'^2})^{1/2}}{U(z)} \tag{6.5}$$

$$i_z = \frac{(\overline{w'^2})^{1/2}}{U(z)} \tag{6.6}$$

where i_y and i_z are the turbulence intensities (non-dimensional), u' is the longitudinal fluctuation velocity, v' is the transverse fluctuation velocity, and w' is the vertical fluctuation velocity. Measurements by Panofsky (1967) revealed for a neutral surface layer that

$$(\overline{u'^2})^{1/2} = 2.2u_* \tag{6.7}$$

$$(\overline{v'^2})^{1/2} = 2.2u_* \tag{6.8}$$

$$(\overline{w'^2})^{1/2} = 1.25u_*. \tag{6.9}$$

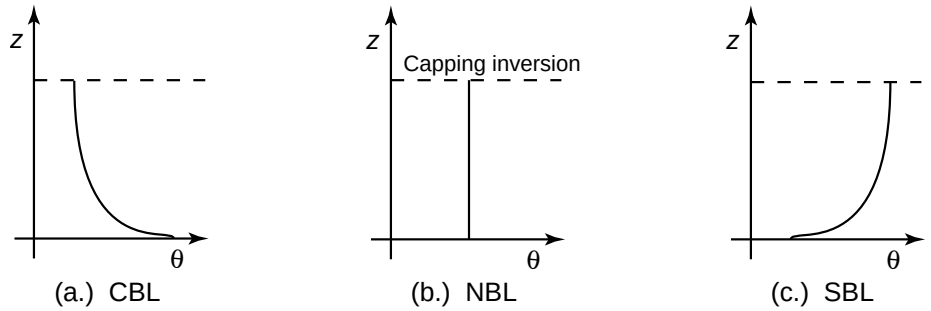

Fig. 6.4. Potential temperature, θ, profiles in the APBL for the three main stability classes: (a.) the convective boundary layer (CBL), (b.) the neutral boundary layer (NBL), and (c.) the stable boundary layer (SBL).

Combining these relationships with the log velocity profile yields

$$i_x = i_y = \frac{0.88}{\ln(z/z_0)} \tag{6.10}$$

$$i_z = \frac{0.50}{\ln(z/z_0)}. \tag{6.11}$$

It is important to note that these data were collected under idealized conditions: large fetch, flat ground, and uniform roughness (often prairie grass).

6.1.3 Effects of buoyancy

Unfortunately, the idealized neutral conditions described above are rarely strictly valid. Heating and cooling within the boundary layer result in temperature differences, which equate to density differences; thus, buoyancy effects and stability/instability are important processes in the APBL.

Shown in Figure 6.4, three general stability types are possible. We have already discussed the neutral case, where the density is constant throughout the boundary layer (refer to Figure 6.4(b.)). During the day, solar radiation heats the bottom air, creating an unstable density profile as shown in Figure 6.4(a.). This case is called a convective boundary layer (CBL). The warm air at the bottom rises, due to its buoyancy, creating enhanced vertical velocities. Because of its special kind of instability, convective instabilities are cellular in shape. That is, circular regions of warm upward-moving air, called thermals, are surrounded by layers of cooler downward moving air. This kind of instability can be seen in a pot of water heated on the stove. The third stability type is show in Figure 6.4(c.). At night, the bottom layer cools rapidly, and the boundary layer develops a stable density profile (heavy air below lighter air). This stable density profile damps the turbulence, in particular the vertical turbulent fluctuation velocities, and encourages internal wave motion. Because of the cellular instability structure of the CBL, and internal wave fields of the SBL, these boundary layers have spatially heterogeneous properties.

Despite these complicated and inter-related effects, generalized quantitative results can be obtained for natural boundary layers. Pasquill (1962) suggested a means of predicting the stability type as a function of wind speed, time of day, and radiative conditions (in

Table 6.1. Pasquill stability categories taken from Csanady (1973).

Surface wind speed in [m/s]	Solar insolation			Night conditions	
	Strong	Moderate	Slight	mainly overcast or $\geq 4/8$ low cloud	$\leq 3/8$ Low cloud
2	A	A–B	B	–	–
2-3	A–B	B	C	E	F
3-5	B	B–C	C	D	E
5-6	C	C–D	D	D	D
6	C	D	D	D	D

A - Extremely unstable, B - Moderately unstable, C - Slightly unstable, D - Neutral, E - Slightly stable, F - Moderately stable.

Table 6.2. Typical turbulence intensities near the ground level, taken from Csanady (1973)

Thermal stratification	i_y	i_z
Extremely unstable	0.40–0.55	0.15–0.55
Moderately unstable	0.25–0.40	0.10–0.15
Near neutral	0.10–0.25	0.05–0.08
Moderately stable	0.08–0.25	0.03–0.07
Extremely stable	0.03–0.25	0.00–0.03

particular, cloud cover, which provides insulation). Table 6.1 provides this stability categorization. Cramer (1959) suggested the associated typical turbulent intensities near the ground level as shown in Table 6.2. As demonstrated in the tables, turbulence intensities are indeed higher in unstable conditions than for stable conditions, and both the vertical and horizontal turbulence intensities are affected.

Combining all these processes, Fedorovich (1999) summarizes the processes affecting mixing as follows:

- large-scale meteorologic forcing (U_0).
- earth's rotation (Coriolis)
- external and internal heating/cooling ($T(z)$)
- physical properties of the surface (z_0)
- physical properties of air (u_*)

The remaining sections incorporate these processes in a description of atmospheric mixing.

6.2 Turbulent mixing in three dimensions

Before we discuss mixing in the atmospheric boundary layer, we should review the turbulent transport equation in a simpler turbulent flow. In Chapter 3 we derived the turbulent advective diffusion equation for homogeneous and stationary turbulence. The transport equation for the mean concentration field C was found to be

$$\frac{\partial C}{\partial t} + \frac{\partial u_i C}{\partial x_i} = D_{x,t}\frac{\partial^2 C}{\partial x^2} + D_{y,t}\frac{\partial^2 C}{\partial y^2} + D_{z,t}\frac{\partial^2 C}{\partial z^2} \tag{6.12}$$

where $D_{i,t}$ are the turbulent diffusion coefficients.

In Chapter 3 we only presented the solutions for times greater than the integral time scale of the turbulence t_I, where we could assume the turbulent diffusion coefficients were constant in time. In general, the turbulent diffusion coefficient in the x direction is given by

$$D_{x,t} = \frac{1}{2}\frac{d\sigma_x^2}{dt} \tag{6.13}$$

where σ_x is the standard deviation of the concentration field in the x-direction (Csanady 1973). Similar relationships are valid for the y- and z-directions. From Taylor's theorem it follows that

$$D_{x,t} = \overline{u'^2}\int_0^t R(\tau)d\tau \tag{6.14}$$

where R is the velocity correlation function of the turbulent flow (Csanady 1973). Generally, we consider two limiting solutions to this equation: at short times for $t \to 0$, and at large times for $t \to \infty$. These solutions are

$$D_{x,t} = \frac{(\overline{u'^2})^2}{\overline{u}}x \quad (x \to 0) \tag{6.15}$$

$$D_{i,t} = (\overline{u'^2})^2 t_L \quad (x \to \infty). \tag{6.16}$$

Thus, the turbulent diffusion coefficients grow linearly at short times until they reach a constant value at times greater than t_L.

Example: Continuous point release. As an example, consider the classical problem of a continuous release at a height h above the ground level. We set the coordinate system so that the mean wind is in the x-direction. The source strength is $\dot{m}$ in [M/T]. To enforce the solid boundary condition at $z = 0$ we use an image source. The solution for the slender plume assumption (diffusion in the x-direction is negligible) is given in Csanady (1973) as

$$C(x,y,z) = \frac{\dot{m}}{2\pi\overline{u}\sigma_y\sigma_z}\left[\exp\left\{-\frac{y^2}{2\sigma_y^2} - \frac{(z-h)^2}{2\sigma_z^2}\right\} + \exp\left\{-\frac{y^2}{2\sigma_y^2} - \frac{(z+h)^2}{2\sigma_z^2}\right\}\right]. \tag{6.17}$$

The solution for the concentration at ground level is given by setting $z = 0$:

$$C(x,y,0) = \frac{\dot{m}}{\pi\overline{u}\sigma_y\sigma_z}\exp\left[-\frac{y^2}{2\sigma_y^2} - \frac{h^2}{2\sigma_z^2}\right] \tag{6.18}$$

and the solution for the centerline of the plume at ground level is given by setting $z = y = 0$:

$$C(x,0,0) = \frac{\dot{m}}{\pi\overline{u}\sigma_y\sigma_z}\exp\left[-\frac{h^2}{2\sigma_z^2}\right]. \tag{6.19}$$

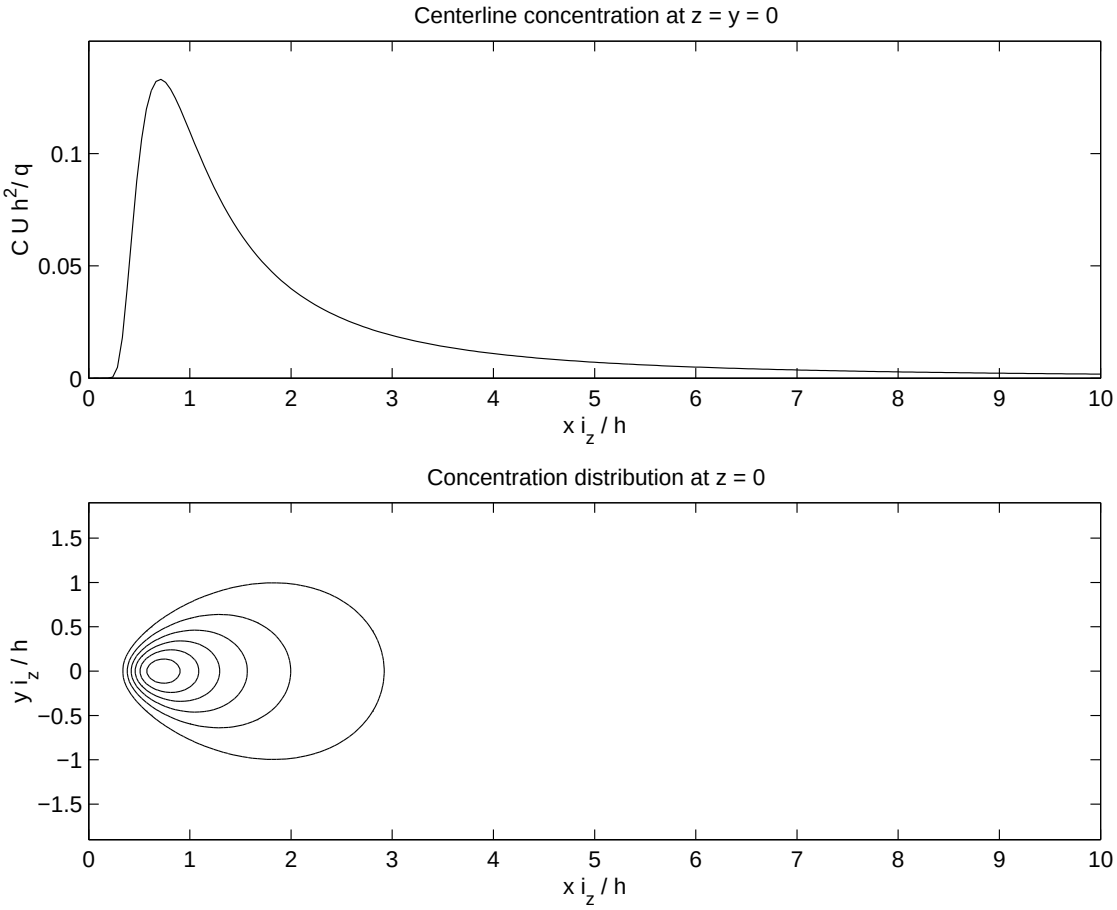

Fig. 6.5. Concentration distributions for a continuous release at a height h into a homogeneous and stationary turbulent flow.

Figure 6.5 shows the solutions of the latter two equations at short times ($t \to 0$) in non-dimensional form.

6.3 Atmospheric mixing models

The results for homogeneous, stationary turbulence are extended in this section to applications in the atmosphere. An underlying assumption for the derivation of (6.12) is that the Eulerian and Lagrangian descriptions of the velocity field are identical. Csanady (1973) points out that this is only true for homogeneous and stationary turbulence if the system is unbounded or bounded by rigid, impermeable walls. The atmospheric boundary layer is indeed bounded from below by a solid boundary, but the top boundary (the capping inversion in Figure 6.2) is permeable. That is, fluid parcels moving in the APBL can move through the capping inversion, bringing high velocity fluctuations with them, and these parcels are replaced by fluid with lower turbulence intensities from above the capping layer. This departure from the idealized case of a solid or semi-infinite boundary results in changes to the velocity correlation function, R, in the APBL. Csanady (1973)

shows, however, that because the solution for the transport equation is insensitive to the shape of the velocity correlation function, this limitation is not dramatic and we will continue to use solutions similar to those in the previous section.

Based on (6.15) and (6.16), we expect different results for short and long times. The processes at short times occur near the source and are called near-field processes. Similarly, the processes at long times occur far from the source and are called far-field processes.

6.3.1 Near-field solution

In the near-field of a release, it is reasonable to assume that the results given above are valid without modification. This is because, at short times, the release has not fully sampled the velocity field and does not know that the turbulence field is bounded by a permeable capping inversion. Hence, the cloud width grows in the near field as

$$\sigma_y = \frac{(\overline{v'^2})}{\overline{v}} x = i_y x \tag{6.20}$$

$$\sigma_z = \frac{(\overline{w'^2})}{\overline{w}} x = i_z x. \tag{6.21}$$

The relationships for the turbulent intensities at a height z were given above. For a release at $z = h$, it is reasonable to use average turbulence intensities. Taking the average from $z = 0$ to $z = h$ gives

$$i_y = \frac{0.88}{\ln(h/z_0) - 1} \tag{6.22}$$

$$i_z = \frac{0.5}{\ln(h/z_0) - 1}. \tag{6.23}$$

Csanady (1973) shows that the near-field solution is valid for a considerable range, often up to the distance where the plume grows so large that is touches the ground, in which vicinity also the maximum ground level concentrations are observed. This is because the Lagrangian time scale is very large, given approximately by

$$t_L = \frac{z_i}{\overline{u}} \tag{6.24}$$

where z_i is the height of the capping inversion.

6.3.2 Far-field solution

Far from the source, the growth of the cloud should depend on the Lagrangian time scale and, due to the shear velocity profile, should be affected by dispersion. Sutton (1932) and Sutton (1953) propose power law formulas for the standard deviations

$$2\sigma_y^2 = C_y^2 x^{2-n} \tag{6.25}$$

$$2\sigma_z^2 = C_z^2 x^{2-n} \tag{6.26}$$

where C_y, C_z, and n are constants, their value depending on atmospheric stability and source height h (Csanady 1973). Under neutral conditions Sutton found the values $n =$

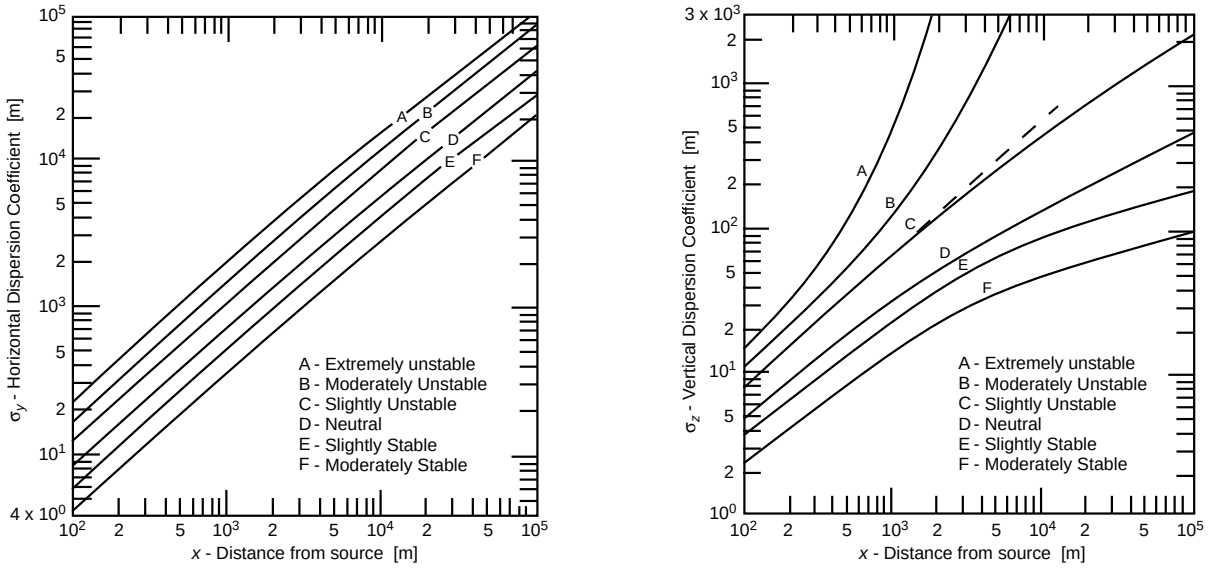

(a.) Horizontal dispersion coefficient. (b.) Vertical dispersion coefficient.

Fig. 6.6. Horizontal (a.) and vertical (b.) atmospheric mixing coefficients. Taken from Csanady (1973).

0.25, while over flat grass-land near ground level he proposed $C_y = 0.4$ cm$^{1/8}$ and $C_z = 0.2$ cm$^{1/8}$ (Csanady 1973). Though this formula is rarely used today, it is important because it represents observed facts.

Under non-neutral conditions, the coefficients introduced above are functions of the stability. Looking first at the *horizontal* growth of the cloud, n has been found to be roughly constant for all stability regimes; C_y is sufficient to adjust σ_y to unstable and stable conditions; and, higher values of C_y are observed in CBLs, and lower values of C_y are observed in SBLs. For *vertical* cloud growth, both parameters are functions of the stability. Figure 6.6 shows the values of σ_y and σ_z for the range of stability classes introduced above. In CBLs, the vertical growth of the cloud becomes vary large due to the large upward velocities of the convective currents. In SBLs, the vertical growth of the cloud is damped due buoyancy effects.

Summary

This chapter introduced mixing in the lower part of the atmosphere, the planetary atmospheric boundary layer (APBL). Turbulence properties in idealized boundary layers were discussed first and then extended to the APBL. The effects of heating and cooling in the APBL result in a range of stability classes, from convectively unstable when heating is from below to stable when cooling is from below. Turbulent mixing in homogeneous stationary turbulence was reviewed and solutions for a continuous source at a height h above a solid boundary were introduced. The results in idealized turbulence were extended in the final section to turbulence in the atmosphere. Simplified atmospheric mixing models were introduced for the near- and far-field cases.

Exercises

6.1 Boundary influence. The effects of a solid boundary are only felt after a plume grows large enough to touch the boundary. Assuming a total plume depth of $4\sigma_z$, find the distance downstream of the release point to where a continuous source release at a height h above a solid boundary first touches the boundary.

6.2 Smoke-stack exhaust. A power company releases 1 kg/s of CO_2 from a height of 30 m into a wind with average velocity 4 m/s. The sky is partly cloudy and the terrain down-wind of the release is pasture land. Estimate the turbulence intensities and find the maximum concentration at ground level downstream of the release. How do the results change if the release point is lowered by 15 m?

6.3 Urban roughness. The results presented in this chapter were for surfaces with uniform roughness and elevations much greater than the roughness height z_0. How do you expect relationships for turbulence intensity to change near the street level in an urban setting (where the roughness is largely due to buildings and houses)?